Hera CubeSats operational mission analysis and trajectory design around binary asteroid for small bodies characterization

A.Felin[*(1)], **P.Annat**[(1)], **J.Vernière**[(1)], **R.Pinède**[(1)], **A.Moussi**[(1)],
M. Rebelo[(2)], **F.Topputo**[(3)], **V.M.Moreno Villa**[(4)]

[1] *Centre National d'Etudes Spatiales (CNES), 31400 Toulouse, France.*
[*]aurelien.felin@cnes.fr

[2] *ISAE-SUPAERO, 31400 Toulouse, France.*

[3] *Politecnico di Milano, 20156 Milan, Italy*

[4] *GMV, 28760 Madrid, Spain*

April 22, 2024

Abstract

The Asteroid Impact Deflection Assessment (AIDA) mission, a collaborative effort for Planetary Defense, involves the DART and Hera spacecrafts targeting the Didymos-Dimorphos binary asteroid system. Their objectives include assessing asteroid deflection, conducting close observations, and demonstrating future mission technologies. DART, launched by NASA, impacted Dimorphos in September 2022, while Hera, an ESA spacecraft, carrying Juventas and Milani CubeSats, is set to reach Didymos in December 2026 after a two-year Cruise phase. The French Space Agency (CNES) contributes to Hera's mission through CubeSats flight dynamics and operations. Both CubeSats will carry out operations in very close proximity to the system including ejection, far range, close range, and landing/disposal phases. The paper presents trajectory designs to fulfill mission programming and flight dynamics operational concepts for Milani and Juventas, highlighting the planning required for the mission's success.

1 Introduction

In the frame of the Asteroid Impact Deflection Assessment (AIDA), an international collaboration for Planetary Defense, the Double Asteroid Redirection Test (DART) and Hera spacecraft will target the binary asteroid system Didymos-Dimorphos. The scientific objectives of the two missions are to assess the deflection of an asteroid, perform close observations for asteroid characterization, and demonstrate technologies for future missions. The first NASA mission, DART, has impacted Dimorphos in September 2022. The second one, Hera, is an ESA spacecraft carrying two European CubeSats (Juventas and Milani) to be launched in October 2024. Hera will have a two-year cruise phase, under ESA/ESOC operations lead.

When arriving close to the binary asteroid, Hera, the mothercraft, will first characterize the asteroids in terms of dynamics, shape, and gravity models, before the release of the two CubeSats: Milani and Juventas. The French Space Agency, CNES, was granted responsibility for close proximity flight dynamics and mission planning operations of these two CubeSats around the binary asteroid. This responsibility begins from the ejection of the mothercraft and extends up to the fulfillment of the scientific objectives of the different CubeSats' payloads. These operations will be held in Toulouse at the FOCSE (French Operation Center for Science and Exploration), which is part of the CMOC (CubeSat Mission Operation Center, ESEC, Belgium) with direct exchanges with the HMOC (Hera Mission Operation Center, ESOC, Germany).

The asteroid close proximity observation will consist of a series of phases, for both CubeSats, with ejection and separation, far range, close range, landing, and disposal phases. Taking into account the mission payloads, navigation, and safety constraints for each phase implies specific trajectories and dedicated maneuver strategies. For instance, ASPECT (hyperspectral imager), Milani's main payload, aims to map both asteroids and image DART crater with specific resolutions and phase angles[1]. For JuRa (low-frequency radar), Juventas main payload, the mission constraints lead to the choice of Sun-Stabilized Terminator Orbit (SSTO) at different altitudes, with a station-keeping strategy in a low gravity environment.

---

[1]Sun-Asteroid center-Satellite Angle

This paper will introduce, in section 2, the dynamics of the Didymos system. After a brief Mission overview in section 3, a description of the mission analysis of each CubeSat will be presented in section 4 and section 5. Finally, a focus on the fulfilment of scientific requirements of Milani Mission Analysis regarding its main Payload ASPECT will be presented in section 6.

2 Dynamics in the Didymos System

Didymos 65803 system is composed of two asteroids of different sizes and shapes. At first glance, only the main asteroid - Didymos or D_1 - was discovered by the University of Arizona Observatory in 1996. Its heliocentric orbit is eccentric with an apogee at 2.3 AU and perigee at 1 AU. Hence, its revolution around the Sun takes 770 days. Regarding the moon of the system - Dimorphos or D_2 -, the latter was not discovered before 2003. Indeed, due to the low Signal Noise Ratio, the presence of D_2 was hardly detectable. However, thanks to the recent success of the DART Mission, more precise data are available from the system and discussed in the section below.

2.1 Properties of the Didymos System

The goal of this section is to provide the reader with the physical properties of the Didymos System. These are indicated in Tab-1 and are taken from Didymos Reference Model 5.0[1] provided by ESA. As stated therein, the only properties measured directly through observations (other than the heliocentric ones presented before) are the orbital period and size ratio of Dimorphos with respect to Didymos, their orbital separation, and the rotation period of Didymos. All other properties are inferred from these measured parameters. For conciseness, the 1-sigma errors of these values are available in [1]. Furthermore, these are **pre-DART impact** properties, and these are the ones that are used throughout this work. For an updated version please refer to [2]. Nevertheless, following the DART and LICIACube probe readings, new models are being developed and the present Mission Analysis is currently being updated. To mention just one of the outstanding results, the period of Dimorphos around Didymos has been reduced by $33\min \pm 1.0\ (3\sigma)$ [3].

2.2 Mission Analysis Dynamics

A spacecraft inserted into the Didymos system environment is subjected to four main interactions that, depending on its distance from the barycenter of the system, will have an impact on the dynamics of the spacecraft. The four main forces that will act on the CubeSats around the Didymos system are the gravitational attraction towards D_1, D_2, and the Sun, and the force due to the Solar Radiation Pressure (SRP).

$$\ddot{\mathbf{r}} = \mathbf{a}_{\mathrm{D1}} + \mathbf{a}_{\mathrm{D2}} + \mathbf{a}_{\mathrm{SRP}} + \mathbf{a}_{\mathrm{sun}} \qquad (1)$$

The model used for the SRP is the so-called cannonball model with CubeSats characteristics shown in Tab-2. Regarding the gravitational field of D_1 and D_2, central force,

D_1 properties	
Diameter*	780 m
Extents along principal axes	$832 \times 837 \times 786$ m
Bulk density	$2170\ \mathrm{kg\,m^{-3}}$
Rotation Period	2.26 h
D_2 properties	
Diameter ratio to D_1	0.21
Diameter*	164 m
Extents along principal axes	$208 \times 160 \times 133$ m
Distance to D_1	1190 m
Bulk density	$2170\ \mathrm{kg\,m^{-3}}$
Orbital Period	11.922 h
Rotation Period	11.922 h
Orbital eccentricity	<0.03

Table 1: Asteroid properties. *Diameter of the sphere with the same volume as the asteroid

Sperical Harmonic Expansion (SHE), and Polyhedron models were compared to assess their relevance depending on the distance to the Didymos system barycenter. In Fig-1 below, a comparison between the high-fidelity model and other dynamics is exposed. It can be inferred from this study that, above 1.3km, central force attraction is considered correct alongside with 3b-Sun and SRP. Under this distance, for the landing phase, more precise models are required, and the use of SHE derived from the polyhedral model is used. Note that below the radius of the Brillouin sphere, the SHE becomes unreliable. For D_2, this radius is approximately 104 meters from D_2 center.

	C_r	A [m^2]	m_{sat} [kg]
Juventas	1.5	0.46	11.37
Milani	1.25	0.51	12

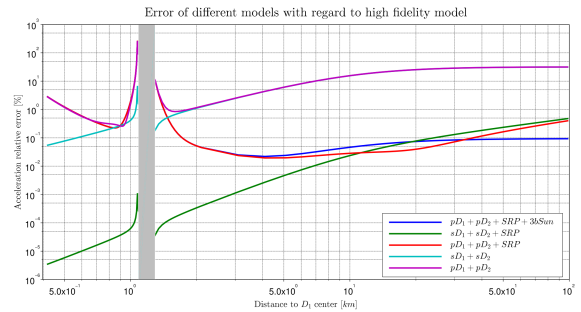**Table 2:** CubeSat Parameters for SRP computation

Figure 1: Comparison between different models of the dynamics near Didymos System. Relative acceleration errors with respect to the high-fidelity model (sD_1 + sD_2 + Solar Radiation Pressure (SRP) + 3b-Sun). Prefix 'p' indicates a point mass model, 's' a SHE of order 5 for D_1 and order 3 for D_2. '3b-Sun' refers to the third body perturbation of the Sun. The grey area corresponds to the range occupied by D_2.

3   Mission overview

This section will present the preliminary mission timeline for both CubeSats and their mothership as well as the hardware of the CubeSats.

3.1   Preliminary Timeline

The launch is expected to happen by the end of 2024 with an arrival in the Didymos system on the 2nd of December of 2026. The two CubeSats will not be immediately released from the mothership. The latter will first perform an Early Characterization Phase to enhance our knowledge of the system. After 6 weeks, the first CubeSat, Juventas will be released on the 16th of January 2027. Fourteen days later, Milani will also be separated from the mothership to start its journey. In Fig-2 and Tab-3 below, the timeline is shown for each spacecraft of the HERA mission.
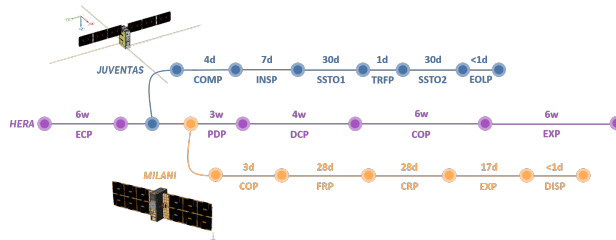

Figure 2: Preliminary Timeline of the HERA spacecrafts where 'w' corresponds to week and 'd' to day. Not to scale.

Juventas		
Preparation Phase	PREP	3 d
Commissioning Phase	COMP	4d
Insertion Phase	INSP	7d
Observation Phase 1	SSTO1	30d
Transfer Phase	TRFP	$1-3$d
Observation Phase 2	SSTO2	30d
End Of Life Phase	EOLP	< 1d
Milani		
Ejection and Separation Phase	ESP	4 d
Commissioning Phase	COP	3d
Far Range Operation Phase	FRP	28d
Close Range Operation Phase	CRP	28d
Experimental Phase	EXP	17d
Disposal Phase	DIP	≈ 1d

Table 3: Juventas and Milani Timeline

3.2   Juventas CubeSat

Juventas is a 6U spacecraft developed by *GomSpace* devoted to the geophysical characterization of Dimorphos. Juventas preliminary mission analysis study has been entrusted to GMV. It is equipped with a low-frequency radar

(JuRa), 3-axis gravimeter (GRASS), radio inter-satellite link (ISL), visible light camera plus Inertial Measurement Unit (IMU). Note that the solar arrays of Juventas are non-rotating. Juventas scientific objectives are to determine the gravity field, interior structure, and surface properties of Dimorphos. The CubeSat aims to operate for a nominal 3-months mission duration, extendable to 6 months, conducting observations within $1-10$km of the target asteroid surface, ultimately concluding with a landing attempt on Dimorphos.
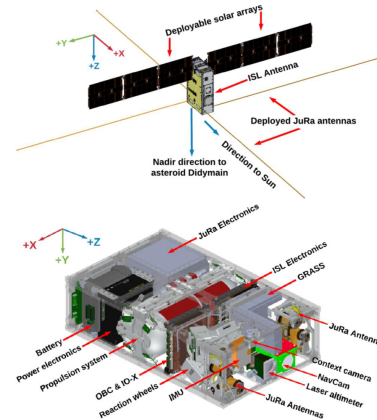

Figure 3: Juventas Assembly

3.3   Milani CubeSat

Milani is a 6U CubeSat developed by *Tyvak International* devoted to the visual inspection and dust detection of Didymos asteroids following DART impact. Milani preliminary mission analysis study has been entrusted to Politecnico di Milano[4][5]. It is equipped with VISTA, a dust analyzer, and ASPECT a multispectral imager to perform mineralogical analysis. In addition to these two main payloads, the satellite is equipped with ISL and a NAVCAM, an opportunity payload originally designed for navigation, but which will serve science too. Note that the solar arrays of Milani are non-rotating, just like Juventas. Milani's main scientific objectives are to map globally the surface of both asteroids, evaluate DART impact effects on D_2, support gravity field determination, and, finally, characterize dust clouds within the binary system. The mission and operational constraints for Milani are mainly derived from the scientific requirements of ASPECT payloads, optical navigation, and ISL. ASPECT requirements will later be detailed in Sect-6.

3.4   Operational Requirements

In addition to their scientific objectives, the two CubeSats are subject to operational constraints arising from their reliance on the Hera mothership. In particular, both CubeSats must maintain proximity within a 60 km range from Hera for effective ISL communications, follow trajectories aligned with the operational team's shifts ($4-3$ days pattern), and ensure the phase angle with respect to Didymos asteroids remains lower than $90°$ for navigation purpose.
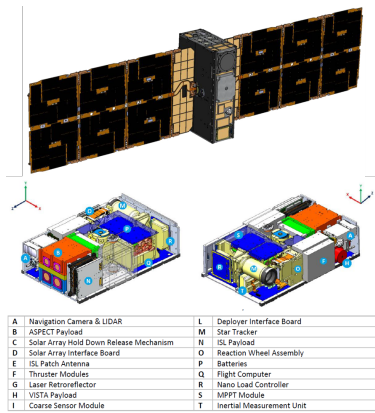
Figure 4: Milani Assembly

4   Juventas Mission Analysis

4.1   Insertion Phase

The Insertion Phase of Juventas is considered the most critical phase of the satellite after landing. Indeed, it represents the first maneuvers performed by the CubeSats in the Didymos dynamics. This phase follows the Commissioning Phase where the CubeSat was released by the mothership and left in free flight. After these 4 days of commissioning, the CubeSat is supposed to reach SSTO1 within 7 days. The design of this phase has been carried out with the idea of being robust to maneuvering errors since calibration will not have been performed yet and given that the dynamics of the system will still be quite uncertain. The phase is designed such that the satellite is injected into a 7-day arc towards SSTO1 through a shooting method. This arc allows a possible maneuver correction after 3 days if the first maneuver was non-nominal. The insertion state on the SSTO1 is determined through a dichotomy process on the Δv spent to reach a final position on the SSTO with true anomaly θ_{SSTO}.
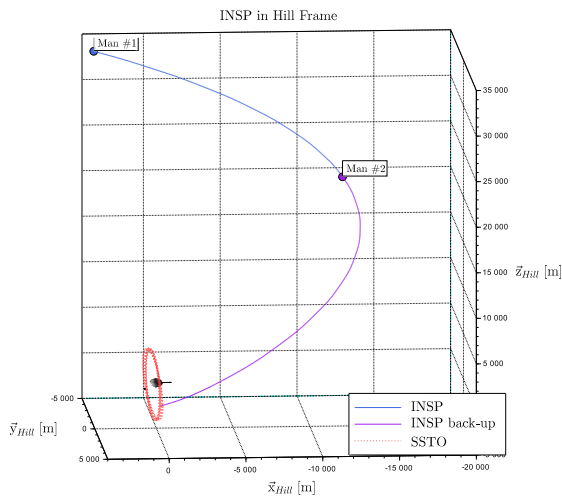

Figure 5: Insertion Phase in Hill Frame

4.2   Sun-Stabilized Terminator Orbit

As exposed in Tab-3, Juventas will pursue most of its scientific missions during the observation phases where the spacecraft will evolve on a SSTO. This type of orbit was chosen for Juventas for its stability. Indeed, in an environment where the SRP is comparable to the attraction forces of asteroids, this choice enables to obtain quasi-periodic orbits. Those orbits have particular characteristics: they belong to a plan normal to the Sun direction and this plan is offset from the barycenter of the system by ten to hundred meters along the Sun direction. Initial conditions for stable orbit can be generated based on the theory developed in [6][7]. Regarding Juventas, it was decided that the satellite will evolve on two successive SSTO with a semi-major axis of 3300 m and 2000 m. Both of them are represented in the Hill frame [2] in Fig-6. The stability of these orbits implies that station-keeping maneuvers are not mandatory. Though, studies are currently undergoing to assess the needs for station-keeping to answer mission programming constraints. Note that the duration of each phase and the altitude considered during preliminary mission analysis could be modified depending on further mission programming optimization studies.
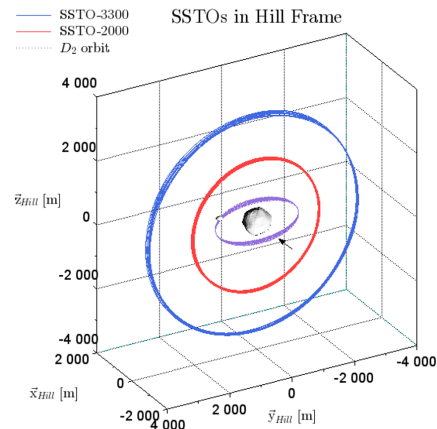

Figure 6: SSTO1 (3300 m) & SSTO2 (2000 m) of Juventas in Hill Frame. Black arrow represents the Sun Direction

4.3   Transfer Phase

The Transfer Phase consists of maneuvering to leave the SSTO1 and reach the SSTO2 as exposed in Fig-7. Studies carried out by CNES have revealed that a modification of the semi-major axis of SSTO1 induces an out-of-plan oscillation of the trajectory that will allow the satellite to intersect the plan of the second SSTO. The two maneuvers are 180° apart and are initially computed using Keplerian hypothesis for semi-major axis modification then tangential correction is adjusted to match the final semi-major

---

[2]X-axis: Anti-sun direction | Z-axis: Parallel to the heliocentric orbital momentum of Didymos |Y-axis: completes the triad

axis. The cost of this transfer is below $4\ \mathrm{cm\,s^{-1}}$ for the complete injection into new SSTO.
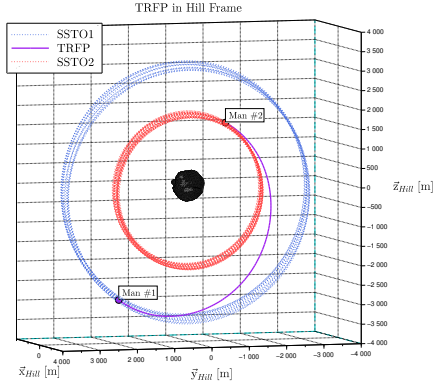

Figure 7: Transfer Phase in Hill Frame

4.4   Landing

Landing on an asteroid is no easy feat, especially on a binary system such as Didymos. Considering a Circular Restricted Three Body Problem (CR3BP) expanded to take into account the ellipsoidal shape of Dimorphos, it is possible to determine the Guaranteed Return Speed (GRS) and an associated Time Of Flight (ToF). The GRS is a necessary condition, from a purely energy perspective, that sets a maximum speed at the surface of D_2 not to be exceeded on landing, at the risk of escaping from the body. The latter is expressed in Eq-2 below.

$$v_{GRS} = \sqrt{2(C^* - U_{\mathrm{eff}}(\mathbf{r}))} \qquad (2)$$

Where C^* is the Jacobi constant of the lowest energy Lagrangian point and U_{eff} is the effective potential taking into account the centrifugal potential of a particle at distance $\mathbf{r}$ from the barycenter of the system. The GRS over DART crater is $4.7 \mathrm{cm\,s^{-1}}$. Thus, velocity at landing must be lower than $v_{GRS}/\eta = 5.875 \mathrm{cm\,s^{-1}}$, where η is the Coefficient of Restitution set to 0.8 (from Rosetta). Regarding the ToF, the latter can be approximated using two-body approximation where D_2 is considered a point mass and D_1 is disregarded. This approximation was checked and it held true near the crater. Knowing the energy of the L_2 point of the Didymos system, it can be found that the zero velocity curve sits around $30\mathrm{m}$ above the crater which corresponds to an approximated $20\mathrm{min}$ free fall time, according to Eq-3 below, assuming the spacecraft departs from rest relative to D_2, at this height.

$$\Delta t_{\mathrm{fall}}^{\mathrm{2BP}} = \frac{1}{\sqrt{2\mu}} \times$$
$$\left[r_2^{3/2} \arctan\left(\sqrt{\frac{r_2}{r_1} - 1}\right) + r_1 r_2 \sqrt{\frac{1}{r_1} - \frac{1}{r_2}} \right] \qquad (3)$$

Where μ is the gravitational parameter of D_2 and (r_1, r_2) are the two distances from the center of D_2 between which to compute the fall time. A preliminary study was carried out relying on a grid search on different landing parameters. These were then converted into candidate trajectories departing from D_2 surface, back-propagated to reach the SSTO using a variable time shooting method. However, this method failed due to high impact speeds exceeding GRS and CubeSat mechanical integrity ($< 10\ \mathrm{cm\,s^{-1}}$). To address this issue, a breaking maneuver was added, enhancing design flexibility. This method divides the landing into two phases: an approach arc bringing the spacecraft closer to D_2 and a descent arc ensuring a safe landing. Assuming the desired landing point is the crater and the initial departure point is somewhere on the SSTO, the method is structured as follows:

1. Backwards propagation of the landing conditions $\mathbf{x}_{\mathrm{land}} = \{\mathbf{r}_{\mathrm{land}}, \mathbf{v}_{\mathrm{land}}\}$ for a time $\Delta t_{\mathrm{descent}}$ resulting in the red trajectory in Fig-8: the **descent arc**. The final position of this backward propagation becomes the position of the breaking maneuver, $\mathbf{r}_{\mathrm{BM}}$.

2. A Lambert arc is computed between $\mathbf{r}_{\mathrm{SSTO}}$ and $\mathbf{r}_{\mathrm{BM}}$ with a time of flight of $\Delta t_{\mathrm{approach}}$ (dashed blue trajectory in Fig-8. Since a Lambert arc is a two-body/Keplerian trajectory, when the initial conditions are propagated in the full dynamic model, the final position of this trajectory, $\mathbf{r}_{\mathrm{BM}}^{\mathrm{Lambert}}$, will not coincide with $\mathbf{r}_{\mathrm{BM}}$. It should, however, not be very far from it, for times of flight which are not too long.

3. A simple forward shooting method takes this arc as an initial guess and corrects the error at the final position $\Delta \mathbf{r} = \mathbf{r}_{\mathrm{BM}} - \mathbf{r}_{\mathrm{BM}}^{\mathrm{Lambert}}$, converging to the solid blue trajectory: the **approach arc**. The shooting method acts only on the initial velocity $\mathbf{v}_0$.

4. The velocity discontinuity between the forward and backward propagated trajectories is then taken as the necessary breaking delta-V $\Delta \mathbf{v}_{\mathrm{BM}} = \mathbf{v}_{\mathrm{BM}}^{+} - \mathbf{v}_{\mathrm{BM}}^{-}$ to connect the two arcs. The velocity discontinuity at the departure position from the SSTO is the necessary departure delta-V $\Delta \mathbf{v}_0 = \mathbf{v}_0 - \mathbf{v}_{\mathrm{SSTO}}$.
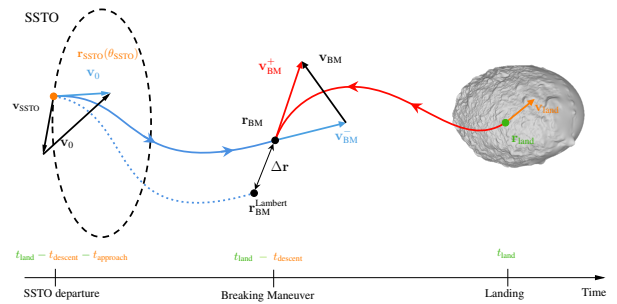

Figure 8: Breaking maneuver trajectory design. The arrows in the trajectory indicate the sense of propagation, **not** of motion.

This strategy produces trajectories with sufficiently low impact speeds. As exposed above, the landing strategy involves five key parameters: landing epoch t_{land}, SSTO departure anomaly θ_{SSTO}, approach and descent times of

flight $\Delta t_{\text{approach}}$ $\Delta t_{\text{descent}}$, and landing velocity v_{land} taken normal to the surface. Finally, an optimizer based on the Nelder-Mead method [8] was implemented which allows for easy implementation of diverse constraints on the trajectory, as well as a selection of different minimization objectives. The initial guess for this optimization algorithm is determined as follows:

- t_{land} : characterization of the position of D_2 is set by the user and the illumination conditions.

- θ_{SSTO} and $\Delta t_{\text{approach}}$: rely on preliminary phasing studies and on illumination condition throughout the landing.

- $\Delta t_{\text{descent}}$ and v_{land}: determined using the three body problem characterization (see Eq-2 and Eq-3).

Below is a possible landing trajectory designed using the method described:
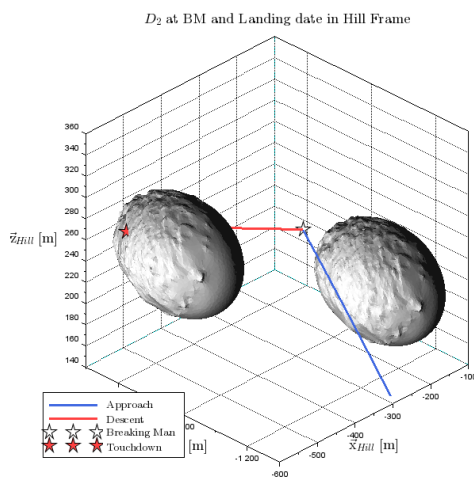

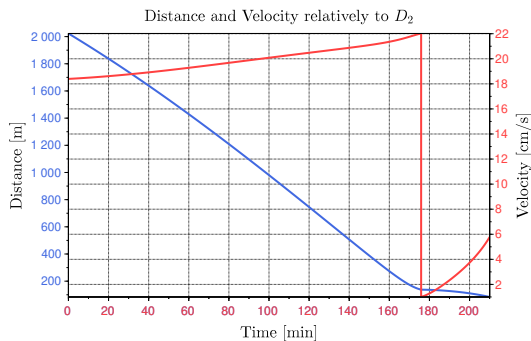**Figure 9:** Juventas Landing. D_2 represented at Breaking manoeuvre (right) and at landing (left)

Figure 10: Distance and velocity with respect to D_2 during EOLP

5 Milani Mission Analysis

5.1 Far Range Operation Phase

The FRP phase aims at observing the system from a distance (~ 10 km) ensuring the safety of the probe and carrying out a complete mapping of D_1 and the first images of D_2 . Its trajectory consists of a succession of hyperbolic arcs on the illuminated side of the two bodies. The maneuvers of this phase are designed to follow the pattern of the Hera probe maneuvers, that is a succession of 4 and 3 days duration arcs. From the scientific requirements, one can define **Waypoints** which correspond to maneuver points in Fig-11. Once these points are defined, a shooting method is used to generate the arcs between the waypoints.
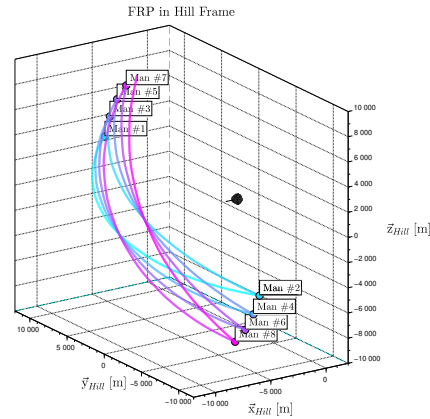

Figure 11: Far Range Operation Phase in Hill Frame

5.2 Close Range Operation Phase

The Close Range Operation Phase goal is to provide a detailed mapping of D_2 , as well as detailed images of the DART crater. The DART crater is set on D_2 surface with a longitude of 264.30 ° and a latitude of -8.84 ° [9]. Two images of the crater at different phase angles have to be acquired. To do so, the phase presents an alternation of three types of arcs: **Waypoint**, **Escape**, **Re-catch**.

Waypoint arcs : These arcs are dedicated to the observations of the crater at specific points of the orbit, called *Keypoints*. These points are set to respect crater imaging requirements mentioned in sect-6. Placing them at such a distance from D_2 is critical and represents a safety risk for Milani which is why they are located around the end of the observation arcs to ensure a minimum time spent at such low distance. These arcs are computed through a shooting method from an initial state to the keypoint position to ensure crater imaging is achieved. Then the state is forward propagated for the remaining ToF of the 7-day arc.

Escape arcs : These arcs are placed right after the waypoint arcs and are designed such that Milani goes quickly and safely away from the system. To determine which direction ensures the safety of the spacecraft, a dispersion analysis is performed for fixed Δv and escape velocity norm (defined as a percentage of the Keplerian parabolic velocity). It is worth pointing out that these maneuvres are the most expensive of the Milani mission analysis due to their close proximity to the system.

Re-catch arc : These arcs are conceived to reach the initial state of the next waypoint arc through a shooting method.
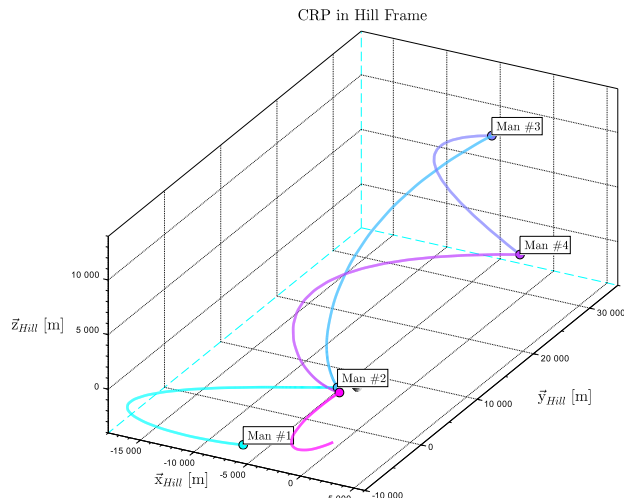
Figure 12: Close Range Operation Phase in Hill Frame

5.3 Experimental Phase

At the end of the CRP, Milani performs a final maneuver to reach the initial position of a 6 km SSTO. There begins the Experimental Phase. The trajectory design is intended to reduce progressively the distance to D_1 to insert Milani into a 3 km SSTO. The method implemented here consists in performing an initial maneuver that will inject the spacecraft into an initial 6 km semi-major axis SSTO (Man1 of Fig-13). This is followed by eight maneuvers spaced $180°$ apart, gradually reducing the SSTO from 6 km to the desired 3 km. It's interesting to note that each maneuver contains two corrections. The first is a correction in Hill's Y-Z plane of the velocity vector, and the second is a semi-major axes reduction maneuver method used in the Keplerian problem.
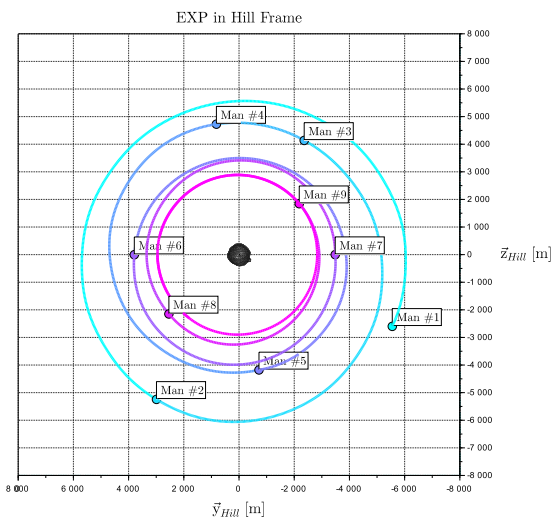

Figure 13: Experimental Phase in Hill Frame

6 FRP-CRP Dedicated Mission

This section focuses on the scientific return of Milani Mission Analysis Design regarding its ASPECT payload. More specifically, the study is performed on the FRP and CRP which are phases where ASPECT requirements drove the design of the mission analysis. ASPECT is a multi-spectral camera designed to map the surface of both asteroids with different phase angles and resolutions. Assumptions made for the analysis, resulting surface mapping of both asteroids and associated mission slots are detailed here below.

6.1 Assumptions

Several assumptions were made for the mapping analysis, including defining the asteroid's Fixed-Frames with z_{FF} oriented towards the pole direction of the associated body, with x_{FF} being arbitrary for D_1 and directed towards D_1 for D_2. The asteroid shape models are given in the Axes-Frames, assumed to be identical to the asteroid's Fixed-Frames. Phase angle calculation is relative to the body's center, not the body's surface, with a small acceptable difference $(1 - 2°)$. The ASPECT camera has a 5-degree half-angle cone for its field of view, and the satellite must observe a zone for at least 5.8 minutes to capture a picture. Criteria for zone visibility include satellites meeting distance and phase angle requirements as well as the absence of eclipses and zone being within the field of view of the camera and being illuminated. Finally, the reader should be aware that this analysis is preliminary and still does not take into account navigation errors that might shorten the mission slots found.

6.2 Mapping Analysis & Mission slots

Mission requirements in terms of resolution are presented in Tab-4. A resolution of 2, 1 and 0.5 m/pix represents, respectively, a distance to the body of $[8.64, 10.94]$, $[1.96, 5.48]$ and $[0.00, 2.78]$ km. The mapping consists of capturing at least five images equally distributed over the longitude while the microstructure consists of imaging a selected area with different phase angles for phase curve measurement. Crater imaging is the riskiest part of the Milani mission, due to the low resolution required, placing the CubeSat at a very short distance from the asteroid. For conciseness, only the results of D_1 mapping during FRP and D_2 crater imaging over CRP are exposed.

		Mapping	Microstructure	Crater Imaging
FRP	D_1	2 m/pix	2 m/pix	–
	D_2	2 m/pix	2 m/pix	–
CRP	D_1	–	1 m/pix	–
	D_2	1 m/pix	1 m/pix	0.5 m/pix

Table 4: Mission to be performed with the associated resolution

7

6.2.1 D_1 **Mapping over FRP**

To properly map D_1, Milani must have a phase angle within $[5, 25]°$ and a distance respecting the 2 m/pix resolution mentioned above. As the FRP, firstly introduced in Fig-11, was designed around ASPECT requirements, its overall mission slots span 31% of the phase duration. As it can be seen in Fig-14, the slots are are distributed around the center of each arc. These slots last for ~ 10.5 and 15.5h respectively for the 3 and 4 day arcs. The resulting mapping of D_1 associated with the mission slots and the ASPECT characteristics are presented in Fig-15. It can be seen that all longitudes of D_1 are covered, making it possible to perform its correct mapping according to scientific requirements.
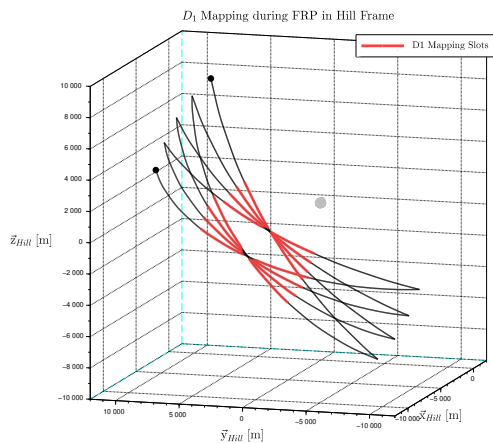

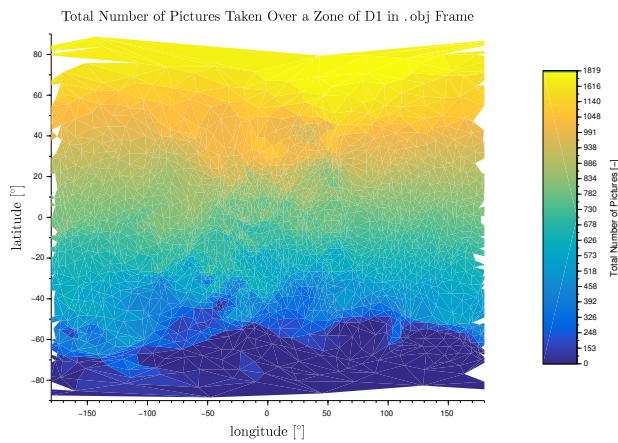**Figure 14:** FRP D_1 mapping in Hill Frame

Figure 15: FRP D_1 mapping in Fixed Frame. Distance $\in [8.64, 10.94]$km and Phase Angle $\in [5, 25]°$ relative to D_1.

6.2.2 D_2 **Crater Imaging over CRP**

As mentioned in sect-5.2, CRP is designed such that Milani can image the DART crater of D_2. The scientific requirements impose to acquire two images of 0.5m/pix

resolution and with different phase angles with respect to the crater. One within $[0, 10]°$ the other within $[30, 60]°$. The first Waypoint arc of Milani is designed to acquire an image with the highest phase angle due to the inclination of the last FRP arc, while the second waypoint arc is designed for the lowest phase angle acquisition. The mission time allocated to both acquisitions is really short due to the great risk of such closeness to D_2. Therefore, the overall dedicated time for crater imaging is only 0.4% ($\sim$2h43min) of the CRP. Regarding mission slots, the $[30, 60]°$ phase angle interval has 2 mission slots: the main one (61min) is, by design, during the first waypoint arc and an opportunity slot (20min) is possible during the second. For the $[0, 10]°$ interval, one mission slot of 40min is available at the end of the second waypoint arc. Therefore, crater imaging as defined by scientific requirements is achievable with Milani CRP trajectory design. In Fig-16, the coverage of D_2 represents the crater imaging requirements associated with phase angle interval $[0, 10]°$.
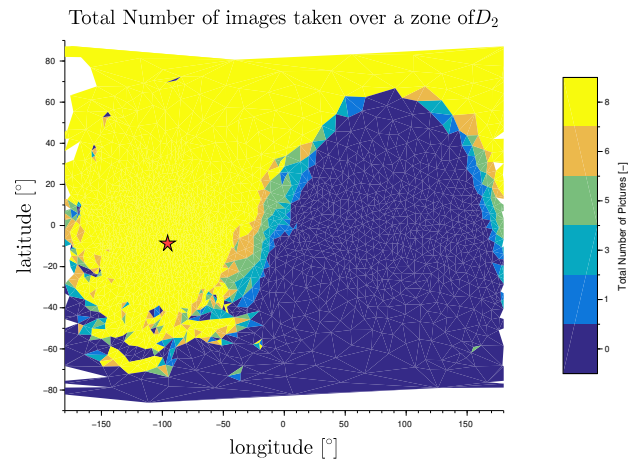

Figure 16: CRP D_2 crater imaging in Fixed Frame with red star representing the position of the crater. Distance $\in [0, 2.78]$km and Phase Angle $\in [0, 10]°$ relative to D_2.

7 Conclusion

In this paper, the reader has been presented with the HERA mission and more especially the Mission Analysis of the two CubeSats, Juventas and Milani, led by CNES. A high-level description of the trajectory design of each CubeSat was presented for each of their phases with the underlying scientific and operational constraints. The latter are strong drivers for trajectory design such as the 3-4 days pattern of the Hera mothership or the coupled distance/phase angle constraints for mission purposes. Finally, a focus on the Milani FRP-CRP trajectory was proposed to the reader with the idea of developing the mission considerations regarding the ASPECT payload. D_1 mapping during FRP and D_2 crater imaging during CRP were studied to assess the viability of the proposed trajectory design. It turned out that both objectives were achievable with a nominal trajectory design.

References

[1] European Space Agency. Hera didymos reference model esa-tecsp-ad-017258.

[2] Cristina A. Thomas, Shantanu P. Naidu, Peter Scheirich, Nicholas A. Moskovitz, Petr Pravec, Steven R. Chesley, Andrew S. Rivkin, David J. Osip, Tim A. Lister, Lance A. M. Benner, Marina Brozović, Carlos Contreras, Nidia Morrell, Agata Rożek, Peter Kušnirák, Kamil Hornoch, Declan Mages, Patrick A. Taylor, Andrew D. Seymour, Colin Snodgrass, Uffe G. Jørgensen, Martin Dominik, Brian Skiff, Tom Polakis, Matthew M. Knight, Tony L. Farnham, Jon D. Giorgini, Brian Rush, Julie Bellerose, Pedro Salas, William P. Armentrout, Galen Watts, Michael W. Busch, Joseph Chatelain, Edward Gomez, Sarah Greenstreet, Liz Phillips, Mariangela Bonavita, Martin J. Burgdorf, Elahe Khalouei, Penélope Longa-Peña, Markus Rabus, Sedighe Sajadian, Nancy L. Chabot, Andrew F. Cheng, William H. Ryan, Eileen V. Ryan, Carrie E. Holt, and Harrison F. Agrusa. Orbital period change of dimorphos due to the dart kinetic impact. *Nature*, 616(7957):448–451, 4 2023.

[3] Cristina A Thomas, Shantanu P Naidu, Peter Scheirich, Nicholas A Moskovitz, Petr Pravec, Steven R Chesley, Andrew S Rivkin, David J Osip, Tim A Lister, Lance AM Benner, et al. Orbital period change of dimorphos due to the dart kinetic impact. *Nature*, 616(7957):448–451, 2023.

[4] Fabio Ferrari, Vittorio Franzese, Mattia Pugliatti, Carmine Giordano, and Francesco Topputo. Preliminary mission profile of hera's milani cubesat. *Advances in Space Research*, 67(6):2010–2029, 2021.

[5] Fabio Ferrari, Vittorio Franzese, Mattia Pugliatti, Carmine Giordano, and Francesco Topputo. Trajectory options for hera's milani cubesat around (65803) didymos. *The Journal of the Astronautical Sciences*, 68(4):973–994, 2021.

[6] Daniel J Scheeres. *Orbital motion in strongly perturbed environments: applications to asteroid, comet and planetary satellite orbiters*. Springer, 2016.

[7] Shota Takahashi and Daniel J Scheeres. Higher-order corrections for frozen terminator orbit design. *Journal of Guidance, Control, and Dynamics*, 43(9):1642–1655, 2020.

[8] J. A. Nelder and R. Mead. A Simplex Method for Function Minimization. *The Computer Journal*, 7(4):308–313, 01 1965.

[9] R Terik Daly, Carolyn M Ernst, Olivier S Barnouin, Nancy L Chabot, Andrew S Rivkin, Andrew F Cheng, Elena Y Adams, Harrison F Agrusa, Elisabeth D Abel, Amy L Alford, et al. Successful kinetic impact into an asteroid for planetary defence. *Nature*, 616(7957):443–447, 2023.

Acronyms

AIDA	Asteroid Impact Deflection Assessment.
CNES	French Space Agency.
COMP	Commissioning Phase.
COP	Commissioning Phase.
CR3BP	Circular Restricted Three Body Problem.
CRP	Close Range Operation Phase.
DART	Double Asteroid Redirection Test.
DIP	Disposal Phase.
EOLP	End Of Life Phase.
ESA	European Space Agency.
ESP	Ejection and Separation Phase.
EXP	Experimental Phase.
FOCSE	French Operation Center for Science and Exploration.
FRP	Far Range Operation Phase.
GRS	Guaranteed Return Speed.
INSP	Insertion Phase.
NASA	National Aeronautics and Space Administration.
PREP	Preparation Phase.
SHE	Sperical Harmonic Expansion.
SRP	Solar Radiation Pressure.
SSTO	Sun-Stabilized Terminator Orbit.
ToF	Time Of Flight.
TRFP	Transfer Phase.